Technical Sciences, 2025, 28, 35–63

UNIWERSYTET WARMIŃSKO-MAZURSKI W OLSZTYNIE

Yearbook peer-reviewed scientific journal
ISSN 1505-4675
e-ISSN 2083-4527
TECHNICAL SCIENCES
Homepage: https://czasopisma.uwm.edu.pl/index.php/ts/

DOI: https://doi.org/10.31648/ts.10781

AN EXPERIMENTAL AND NUMERICAL INVESTIGATION OF PARTICLES FLUID DYNAMIC FLOW AND ENERGY TRANSFER IN A HEAT EXCHANGER PART 1. AN EXPERIMENTAL AND NUMERICAL GRANULAR MATERIAL FLOWABILITY STUDY

***Samkelo M. Khumalo*[1], *Waldemar F. Cieslakiewicz*[2], *Daniel M. Madyira*[3], *Dewald Scholtz*[4], *Jan Serfontein*[5]**

[2]ORCID: 0009-0001-9153-5558
[3]ORCID: 0000-0002-2840-1311
[1, 2, 3]Department of Mechanical Engineering Science
University of Johannesburg, Gauteng, South Africa
[4]Drytech International (Pty) Ltd, Johannesburg, Gauteng, South Africa
[5]Aerotherm (Pty) Ltd, Pretoria, Gauteng, South Africa

Received 11 November 2024, accepted 5 May 2025, available online 6 May 2025.

Keywords: DEM, Hertz Mindlin, Lagrangian multiphase, multiphase interactions, rolling resistance, time step, flowability.

Abstract

Flowability is of great importance to a lot of processes especially granular material handling and heat transfer. In the industry achieving the highest heating efficiency of granular material heat exchanger is the most important factor. Heating/cooling area size is one of the critical factors in heat transfer processes and is highly dependent on flowability. The complexity of optimizing flowability can only be solved in two ways, either through experiment or computational modelling. However, the simulation technique is more time efficient and cost effective compared to the experimental analysis technique. Nonetheless, the CFD methodology requires prior validation of the model with the experiment. This study comprises of the experimental and numerical analysis of granular material flowability, and it aims at establishing a balanced flow of spherical silicon particles in a heat

Correspondence: Waldemar F. Cieslakiewicz, Department of Mechanical Engineering Science, University of Johannesburg, Johannesburg, South Africa, e-mail: waldemarc@uj.ac.za

exchanger and developing a validated model that can be used for design optimisation. A Discrete Element Method (DEM) is employed in Simcenter STAR CCM+ to analyse the flow behaviour and is validated qualitatively and quantitatively from the experimental data. The results from both the simulation and the experiment exhibit a similar trend, indicating consistency between the two approaches. In both cases, the particle velocities are not uniform within the heat exchanger, as variations are observed across different regions, from 2 mm/s to 9 mm/s. Specifically, particles near the heat exchanger walls experience lower velocities due to higher frictional resistance, while those in the central flow stream, especially close to the outlet, move at relatively higher speeds. Quantitatively, the percentage difference between the simulation and experimental results is 9.53% for particle velocity and 5.61% for mass flow rate, which falls within an acceptable range for computational modelling of granular flow. This level of accuracy indicates that the simulation effectively captures the key flow dynamics within the heat exchanger, making it a reliable tool for further analysis. The study shows convincingly that the model was validated successfully, however investigated heat exchanger is highly inefficient but using the validated model can be optimized.

The study comprises two parts. The first one presents the experimental and numerical particles flow analysis of the fluid (granular material), while the second one focuses on the experimental and numerical energy transfer (heating/cooling) analysis.

Introduction

Granular flowability plays a crucial role in numerous industrial processes such as material handling, drying and granular material transportation, just to name a few. However, as stated by FERNANDES et al. (2017), our knowledge of the granular material's mechanics is still lacking and incomplete. For instance, TAHMASEBI (2023), mentions that because of our lack of understanding of granular flowability, 40% of the capacity is estimated to be wasted in industrial operations. As defined by SANTOMASO et al. (2003), granular flowability is the ability of granular particles to freely and consistently flow on a regular basis. Numerous studies have investigated factors that affect flowability of granular materials in different processing devices such as hoppers and rotary drums. Some of these factors include particle surface roughness, ZHANG et al. (2023), angle of repose, BEAKAWI AL-HASHEMI and BAGHABRA AL-AMOUDI (2018), particle size, porosity, particle shape and compressibility, STANLEY-WOOD (2009), just to mention a few.

Experiments conducted with rotary drums provides valuable insight into granular flow particularly in understanding particle mixing and segregation (KHAN, XU 2024). ZHENG and YU (2015) – have studied the flow behaviour of cohesionless granular materials with 100 mm diameter, 2000 kg/m^3 density, 10^6 Pa Young's modulus and 0.3 Poisson's ratio, using the Eulerian method. In this study, they observed a linear particle velocity distribution along the mid-cord of the particle bed, which aligns well with data previously published by BOATENG (1998). Even though the study addresses how wall friction of the drum affects slipping, slumping and rolling of the particles, they do not address how altering particle friction parameters would affect the flowability.

KHAN and XU (2024) have investigated the effects of varying the drum rotational speed, dynamic friction angle and damping ratios on the flowability of granular material of mono-sized and poly-sized particles in rotary drums. The study featured 160 particles with 40 mm diameter, 700 mm particles with 25 mm diameter,

ad 2 800 particles with 14 mm diameter. It was observed that higher rotational speeds cause particles to collide more frequently thereby rearranging them where larger particles, due to their higher inertia, resist centrifugal force and tend to remain near the outer edges of the system, and smaller particles experience a stronger relative centrifugal force, causing them to migrate toward the center. They also observed that increasing the damping ratio enhances particle cohesiveness and frictional resistance, leading to reduced segregation and slower velocities. However, the study does not address the effects of shape irregularity on the flowability as well as varying particle friction factors.

JIAN and GAO (2023) have investigated the flow behaviour of differently shaped particles (spherical, non-spherical and their mixtures) in a flat-bottomed hopper with vertical walls. Their study looks at plastic ball, mung bean, wooden cylinder, wooden ball, wooden cubic and plastic cylinder particles with diameters ranging between 4-6 mm, length for cylindrical and cubic particles ranging between 5-8.5 mm, and density ranging between 476-1592 kg/m^3. The results indicated flat bottomed hoppers do not completely discharge but form an inclination angle at which particles settle relative to the corners of the hopper. The results also indicated that the discharge rate of a binary mixture does not always lie between the discharge rates of the two single-component particle systems, but if the properties of particles in a binary mixture are similar, then their residual inclination angles. However, this study does not consider the effects of inclining the angles of the hopper on the particle flow behaviour.

On the other hand BALEVIČIUS et al. (2011) have investigated the flow patterns of pea grain with diameter ranging between 30-35 mm, density of 500 kg/m^3, Elastic modulus of 0.3 MPa and Poisson's ratio of 0.3 in differently shaped hoppers. Their study looked at flat bottomed, space-wedged and plane wedged hoppers with a fixed outlet size. 1980 particles were filled in each hopper while the bottom was closed and left to discharge by opening the outlet and allowing particles to free fall. They observed that a plane wedged hopper discharges faster compared to the other hoppers, whereas a space wedged hopper creates space retarded flow where particles dissipate their kinetic energy through contact. In these types of hoppers, particles have more contact with each other and their surroundings. They also observed that the flat-bottomed hopper does not completely discharge as some particles form a stagnation region along the corners. Although this study addresses how different wedged shapes affect the flow behaviour, it does not address the effects of varying particle and wall friction factors on the flow behaviour. It does not look at how different particle shapes would affect the flowability in these hoppers.

Based on the aforementioned studies, it is clear that the dynamic behaviour of granular materials can be analysed in two ways. Either through experiment or computational modelling. However, the simulation technique is more time efficient and economically advantageous when compared to the experimental

analysis technique. As stated by BALEVIČIUS et al. (2011), the Discrete Element Method (DEM) is the most widely used tool for analysing granular materials, as it offers a detailed understanding of the individual particle behaviour and the interparticle forces acting between them. SHI et al. (2024) states that Hertz--Mindlin is the default model when simulating in DEM. The model consists of tangential and normal forces (MINDLIN, DERESIEWICZ 1953), namely (Siemens Digital Industries Software 2023):

– coefficient of rolling resistance;
– static friction coefficient;
– tangential restitution coefficient;
– normal restitution coefficient.

These values are determined through experiments to accurately simulate a realistic scenario. Is indicated by AELA et al. (2022), the static friction coefficient can be determined using the angle of repose. MCGLINCHEY (2008) defines the angle of repose as the angle formed between the slope of granular material that is dropped a known height and the horizontal plane. The relationship between the angle of repose and the static friction coefficient is given by BEAKAWI AL-HASHEMI and BAGHABRA AL-AMOUDI (2018) as shown in following equation.

$$\mu_s = \tan\theta \tag{1}$$

where:

θ – the angle of repose,
μ_s – the coefficient of static friction.

In this study, a computer simulation based on Discrete Element Method (DEM) is used to analyse the flowability of granular material in a plane-wedged hopper heat exchange. An experiment is conducted to determine reference values for the DEM setup. The study will look at factors affecting flowability of granular material in a heat exchanger, then alter the factors to optimise the heat exchanger design.

Experimental and Numerical Study of Granular Material Flowability in the Heat Exchanger

The aim of this study is to experimentally investigate the flowability of silicon particles in a plane wedged stainless steel heat exchanger that has a fixed opening and use the obtained results to develop a numerical model. The study determines the factors that affect the flowability and use the factors to optimise the design of the heat exchanger.

Theoretical Background

Calculations of particles physical parameters

Calculation of material density is carried out by the following formula:

$$\rho_b = \frac{m_t}{v_t} \tag{2}$$

where:

m_t – the mass of the weighed particles,
v_t – the volume of particles,
ρ_b – the bulk density of the particles.

The volume of the particle is guided by the equation:

$$V_p = V_p = \frac{4}{3}\pi r_p^3 \tag{3}$$

where:

V_p – the volume of the particle,
r_p – the radius of the particle (the diameter of the particle is 4 mm).

The number of particles the heat exchanger occupies is calculated by the formula:

$$n = \frac{V_T \cdot \eta}{V_p} \tag{4}$$

where:

η – the packing density fraction of the particles.

The particle velocity at different areas of the heat exchanger were calculated by the equation, as follows:

$$\vartheta = \frac{\Delta L}{t} \tag{5}$$

where:

v – the velocity of the particle,
ΔL – the distance travelled by the particle and is given as ($\Delta L = L2 - L1$),
t – the time taken by the particle to travel through the distance ΔL.

Moment of inertia of the particle, with Newtons second law, the rolling resistance formula μ_R was derived to be:

$$\mu_R = \frac{a}{2g\cos\theta} \tag{6}$$

where:

μ_R – the rolling resistance coefficient of friction,
a – the acceleration of the particle,
g – the gravitational acceleration,
θ – the inclination angle of the angle iron rod.

The acceleration of the particle is determined using the kinematic equation as follows:

$$\Delta s = v_i t + \frac{1}{2} a t^2 \tag{7}$$

where:

v_i – the initial velocity and is zero,
t – the average time taken for the particle to roll down,
Δs – the overall length of the stainless-steel angle.

$$a = \frac{2\Delta s}{t^2} \tag{8}$$

Model meshing

Polyhedral meshes provide a balanced solution for complex mesh generation problems. They are relatively easy and efficient to build and occupy less discretized entities considering other traditional meshing approaches like tetrahedral and hexahedral considerations. The polyhedral meshing model utilizes an arbitrary polyhedral cell shape in order to build the core mesh. In Simcenter This mesh is constructed from an underlying tetrahedral mesh, utilizing a unique dualization scheme. The polyhedral cells that are created typically have an average of 14 cell faces. This high face count improves cell face-to-centroid orthogonality, which benefits this case by providing the capability for higher-order flow capturing.

Source smoothing using cell clustering is an important consideration in situations where high-density DEM flow is present. The solver requires a volume fraction of less than one, concerning polyhedral cell volume and particle volume, to both resolve particle trajectory and flow determination. Simcenter STAR-CCM+ resolves this high-density DEM flow by employing source smoothing using cell clustering. This mechanism spreads the effect of large particles across multiple cells, hence resulting in a lowered volume fraction while maintaining gaseous flow resolution in the background mesh.

DEM model

Discrete Element Modelling (DEM) is a method to predict the interaction between discrete particles, particularly in cases where particle-particle interaction dominates the macro behaviour of a system. In this case, DEM is well suited to predict the many inter-particle interactions and particle-wall interaction as the ore particles into the experimental domain. DEM, however, can be very computationally intensive as each particle interaction must be calculated at every time step as the simulation progresses through time. To greatly save computational time, though, a mesh-less approach could be considered. This assumption only holds in scenarios where the gaseous phase has minimal influence on the particulate phase. This however is not the case for the simulation considered, there for a more traditional approach is considered with a well-defined background poly-dominant mesh.

Multiphase interaction model

The results of a DEM simulation leverage heavily on specific particle--dependent properties. Before a simulation is to be completed, a thorough investigation is to be conducted to determine:

– Tangential and normal Restitution coefficients;
– Static Friction coefficients;
– Youngs Modulus;
– Possible particle cohesion.

These values should be tuned to closely correlate with an experimental setup. This will then enable a high order of accuracy considering particle-particle interactions as well as particle-wall interactions.

The Hertz-Mindlin model is a commonly used contact model used to define particle and particle-wall interactions. This model is employed to simulate the contact behaviour between particles, taking into account the elastic and non--elastic components of the contact force.

Experimental study of granular material flowability in the heat exchanger

Equipment description

The numerical modelling of the heat exchanger to study the energy transfer from heating elements to the granular material requires knowledge of the particle's movement inside the exchanger. A dedicated test rig was designed and built by Drytech International (Pty) Ltd to test the material flow behaviour inside

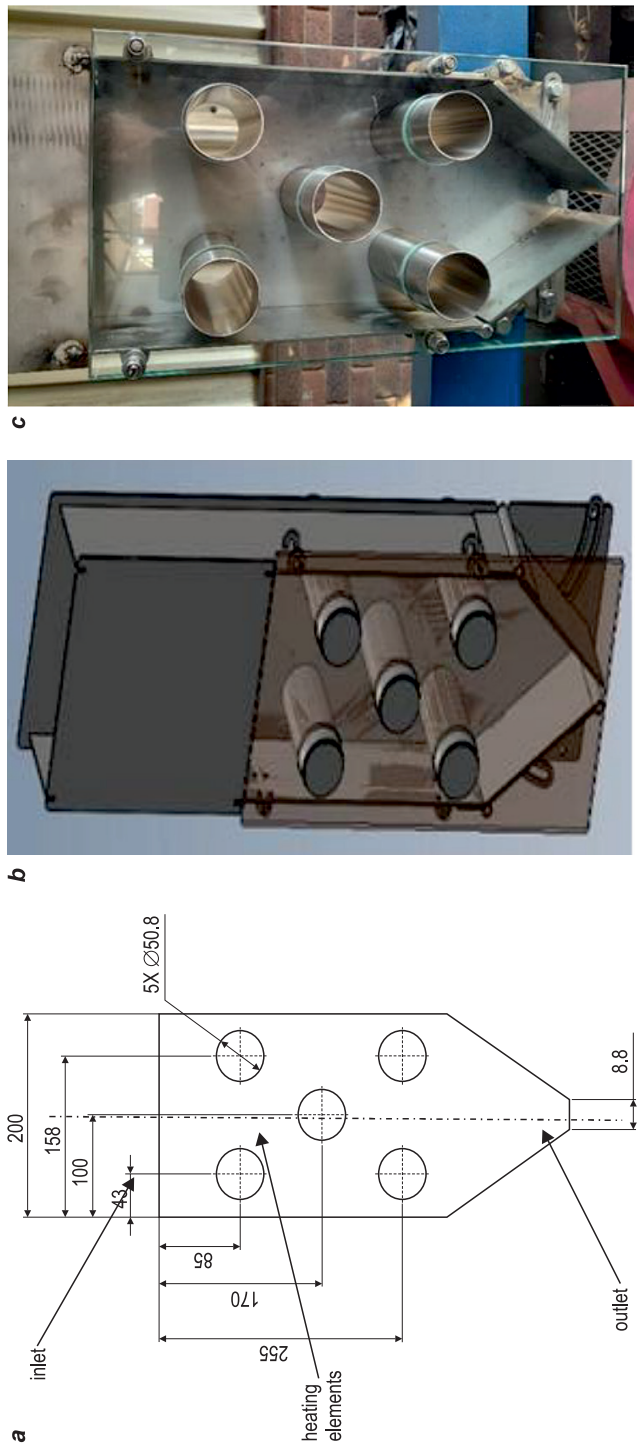

Fig. 1. Heating/cooling exchanger: *a* – dimensions, *b* – design isometric view, *c* – test rig view
Source: Drytech International (Pty) Ltd

the exchanger. The dimensions of the developed device are shown in Figure 1*a*, an isometric view of the device in Figure 1*b* and the prototype of the test rig in in Figure 1*c*. The heat exchanger takes shape of the plane-wedged hopper which is made from 2205 stainless steel and glass wall (to facilitate observation) on one side. The overall dimensions of the heat exchanger were 430 mm length, 80 mm depth, 200 mm width, and adjustable outlet, which for this experiment was fixed at 80 by 8.8 mm. Later shown, a tape measure was placed on the side of the heat exchanger to help measure the distance travelled by the particle. To ensure precision, a digital camera is employed to capture the dynamic flow of particles. The recorded footage is then analysed to determine particle velocities at various sections of the heat exchanger by measuring the time taken for particles to move between specific points. In this set up, the heat exchanger was fixed to a frame, leaving sufficient space between the outlet and the ground, to let the particles flow easily under the influence of gravity. The geometry also features five tubes at the positions indicated in Figure 1 that are to be fitted with the heating elements during the energy transfer experiment. At this stage of research (particles flow movement), the tubes are replaced with 2205 stainless steel cylinders. The particles are loaded into the heat exchanger at the top, through the inlet and are at discharged at the bottom through the outlet.

Material description

In this study, mono-sized spherical silicon particles with 4 mm diameter, 112 GPa Young's modulus and 0.28 Poisson's ratio (MatWeb 2024) were used as the experimental material. Particles were coloured with four different colours (mainly brown, blue, green and white) prior to the experiment to enhance visualization and tracking of flow behaviour within the heat exchanger. This approach allows for a clearer distinction between different flow regions, stagnant zones, and velocity variations. This colour variation method helps improve the accuracy of flowability assessments, since the trends are easily observable. Other properties of the material, mainly the friction factors, had to be determined with an aid of experiment.

Particles size distribution

Material particles size of granular material generally is described in the form of normal particle size distribution (PSD) known as log-normal distribution, shown in Figure 2, based on Gaussian distribution, where x axis represents particles size and y axis represents volumetric/mass percentage of particles passing specific size in total volume/mass. The material in this experiment has PSD = 100 because all particles have the size = 4 mm.

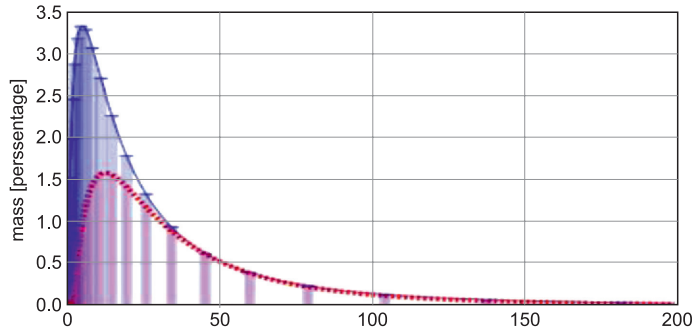

Fig. 2. PSD of granule material

Calculation of the material bulk and specific density

Silicon particles with the average diameter of 4 mm was the granular material under this study. Through the experiment, the bulk density ρ_b, which as defined by KUMAR (2023), is the mass per unit overall volume occupied by the material (where the volume includes voids) was calculated by formula, Equation 2.

The calculation process was conducted as follows:

1. A certain amount of particles was weighed inside a glass beaker as shown in Figure 3. The beaker was weighed first, so that its mass is removed from the total weight of the silicon particles.

Fig. 3. Weighing the silicon particles
Source: Drytech International (Pty) Ltd

2. Next the volume of particles in beaker was measured by reading a scale on the beaker.

The weighed mass m_b of the silicon particles in the beaker was:

$$m_b = 1095.7 \text{ g.}$$

The measured volume v_b of the particles in the beaker was:

$$v_b = 500 \text{ ml.}$$

Therefore, the bulk density ρ_b of the silicon particles calculated by formula, Equation 2 becomes:

$$\rho_b = \frac{1095.7}{1000 \cdot 500 \cdot 10^{-6}} = 2191.4 \text{ kg/m}^3.$$

The specific density of the material was calculated in the following way. The beaker with particles inside was slowly filled with the water to level of particles occupied beaker. The amount of water v_w used was 198 ml.

The weighed mass of the silicon particles in the beaker was still the same:

$$m_s = 1095.7 \text{ g.}$$

The volume v_s of the particles in the beaker this time was:

$$v_s = v_b - v_w = 500 - 198 = 302 \text{ ml.}$$

Using the formula, Equation 2 we can calculate the specific density ρ_s of the material:

$$\rho_s = \frac{1095.7}{1000 \cdot 302 \cdot 10^{-6}} = 3628.14 \text{ kg/m}^3.$$

Measurements of the material angle of repose

The angle of repose, which as defined by MCGLINCHEY (2008) is the angle that is formed by a pile of the granular particles on a horizontal platform, was measured to be 15°. The process of measuring the angle of repose requires that particles are dropped from a certain height onto a flat surface and then measure the pile angle. However, the spherical particles were difficult to contain at a single area, since they roll. To successfully obtain the angle of repose, a cylindrical pot was used to constrict the particles from rolling around as seen Figure 4, where only the piled part was measured. Based on Carr classification of flowability (BEAKAWI AL-HASHEMI, BAGHABRA AL-AMOUDI 2018), angle of repose lesser than 30° implies that the material is very free flowing.

Fig. 4. Measuring the angle of repose
Source: Drytech International (Pty) Ltd

Calculation of rolling resistance coefficient

An experiment to find the coefficient of rolling resistance was performed, where a 1319 mm long stainless-steel angle iron bar was placed at an angle of 2.7° is shown in Figure 5. In this experiment, a silicon particle with a diameter of 4 mm is released and left to roll down the length of the bar. The time taken for the particle to roll down along the length of the bar is recorded. The experiment was done 10 times, and the results were averaged for accuracy.

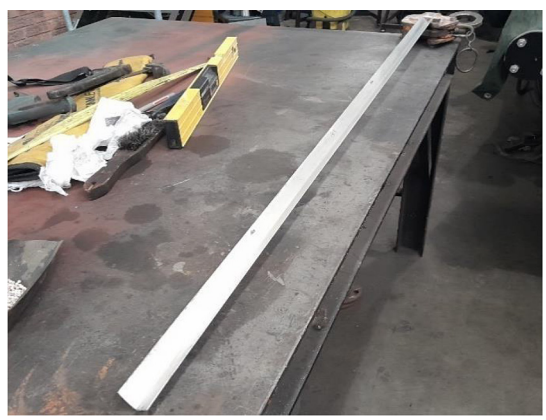

Fig. 5. Experimental set up for rolling resistance calculation
Source: Drytech International (Pty) Ltd

The averaged time was 11.60 seconds. Through the application acceleration was calculated by formula, Equation 8 and the rolling resistance was calculated by formula, Equation 6.

$$a = \frac{2 \cdot 1.319}{(11.6)^2} = 0.0196 \text{ m/s}^2$$

$$\mu_R = \frac{0.0196}{2(9.81)\cos(2.7)} = 0.001$$

Experimental procedures

The order of the experiment follows the determination of flow profiles, particle velocities and finish with particle mass flow rate. To achieve this, the procedures followed include:

– calculation the number of particles in heat exchanger;
– measurements of particles flow rate;
– measurements of particles velocities in selected areas of heat exchanger.

Calculation the number of particles in heat exchanger. For the flowability of granular materials test, the heat exchanger is filled with differently coloured particles as seen in Figure 6. To calculate the number of particles that the heat exchanger can retain, the volume of the heater exchanger and the volume of a single particle were used. The volume of the heat exchanger V_t is calculated by the formula, Equation 9.

For simplification, a single rectangular prism with empty spaces is assumed. The empty spaces include the 5 cylindrical holes and the two triangular spaces at the bottom of the test rig.

V_T = volume of solid – volume of empty spaces

$$V_T = L \cdot W \cdot H - 5 \cdot \pi r_e^2 x - 0.5 \cdot 2 \cdot b \cdot h \cdot l \tag{9}$$

where:

L – overall length of the heat exchanger,
W – overall width of the heat exchanger,
H – overall height of the heat exchanger,
r_e – the radius of the radius of the heating elements,
x – the height of the heating element (equal to the width of the heat exchanger),
b – the base edge of the triangular section,
h – the height of the triangular section,
l – the length of the triangular section.

Fig. 6. The heat exchanger filled with particles
Source: Drytech International (Pty) Ltd

$$V_T = 200 \cdot 80 \cdot 430 - 5 \cdot \pi(25.4)^2(80) - 0.5 \cdot 2 \cdot (95.6) \cdot (80) \cdot (130),$$

$$V_T = 5.075028033\text{E}^{+6}\ \text{mm}^3.$$

Figure 7 shows the calculated volume of the heat exchanger through Solidworks, which corresponds to the calculated volume above.

Volume = 5075028.03 cubic millimeters
Surface area = 281235.61 square millimeter

Fig. 7. Volume of the heat exchanger calculated through Solidworks Software

The volume of the particle is obtained using the formula, Equation 3:

$$V_p = 33.51\ \text{mm}^3.$$

The number of particles that the heat exchanger occupies is calculated by the formula, Equation 3: Packing density measures how efficiently granular particles fill up the space within the given volume. As stated by KALLUS (2016), for spherical particles with the same size, the packing density for random packing is approximately 64%, whereas HAO (2008) approximates it to 63%. Therefore, assuming the packing density of 63%, the number of particles in the heat exchanger is approximated to n=95,413 by using the formula, Equation 4:

$$n = \frac{5.075028033E^{+6} \cdot 0.63}{33.51}$$

$n \approx 95{,}413$ particles.

Measurements of particles flow rate. To determine the mass flow through the heat exchanger, three runs of flow measurements were conducted, each containing five experiments for accuracy. The averaged measurements are presented in Table 1 and the graph of mass flow for all runs is depicted in Figure 7. It was calculated that the mass of one particle is 0.07343 g and the average material weight for all runs is 140.8 g/s, which results in a flowrate of 1917 particles/sec flowing out of exchanger.

Table 1

Mass flow rates measurements

Runs	Average mass [g]	Average flow time [s]	Average flow rate [g/s]
Run 1	4398.27	30.83	142.65
Run 2	3951.96	28.1	140.64
Run 3	3950.72	28.4	139.11

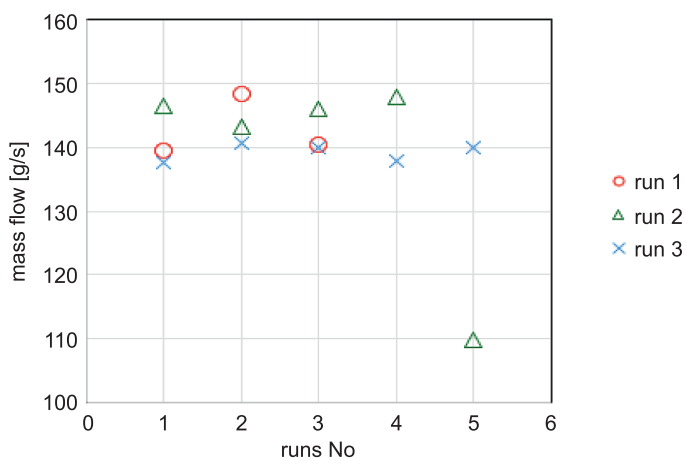

Fig. 7. Mass flow rates through the heat exchanger

Measurements of particles velocities in selected areas of heat exchanger. A tape measure is affixed to the side of the heat exchanger (on the glass side), as illustrated in Figure 8. To ensure precision, a digital camera is employed to capture the dynamic flow of particles. The recorded footage is then analysed to determine particle velocities at various sections of the heat

exchanger by measuring the time taken for particles to move between specific points. To facilitate the observation of velocity profiles, the heat exchanger is filled with particles in four distinct colours, as depicted in Figure 8. Figure 8 shows particles that are initially stationary and then when they begin flowing. The observations reveal that particle flow rates differ across sections of the heat exchanger, with some areas experiencing lower resistance than others.

Fig. 8. Depictions of granular material movement in the heat exchanger
Source: Drytech International (Pty) Ltd

Particle velocity is an important parameter which characterises the flow. In the heat exchanger experiment, four areas were identified to measure particle velocity. These four areas are identified and named as presented in Table 2.

Table 2

Naming of areas for velocity measurements, see Figure 9

Symbol	Name
a	area between two lower tubes
b	area between two top tubes
c	area between lower right tube and the wall
d	area between the top right tube and the wall

For the sections listed in Table 2, a particle is tracked as it moves between two points, $L1$ and $L2$, while recording the time taken to travel between them. $L1$ serves as the starting point, and $L2$ is the endpoint. The time required for the particle to flow from $L1$ to $L2$ is carefully measured and recorded. The distance, L, is measured from the start of the glass wall to the outlet, as marked by the tape measure. Table 3 presents the experimental results, while Figure 9 illustrates how the video was utilized to determine both the travel time and the distance covered by the particle.

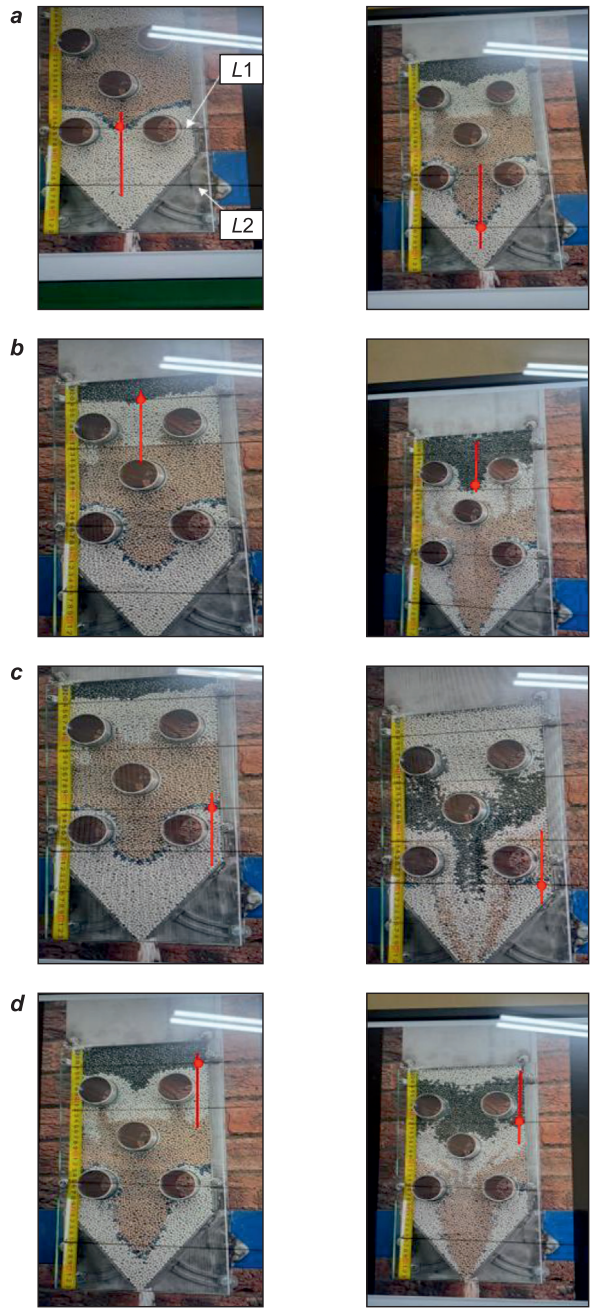

Fig. 9. Photographic frames of granular material flow: *a* – channel between two lower tubes, *b* – channel between two top tubes and *c* – channel between lower right tube and the wall, *d* – channel between top right tube and the wall
Source: Drytech International (Pty) Ltd

Table 3

Distance and time taken for the particle to flow between two points across the heat exchanger

Area	$L1$ [mm]	$L2$ [mm]	Time [s]	Velocity [mm/s]
a	252	352	11	9.09
b	40	122	12	6.83
c	220	290	43	1.63
d	40	122	15	5.47

The particle velocity at different areas of the heat exchanger were calculated by the formula, Equation 5. As a sample calculation the velocity in area (*a*) is calculated as:

$$\vartheta = \frac{L_2 - L_1}{t} = \frac{352 - 252}{11} = 9.09 \text{ mm/s}.$$

Through observations from Figure 7, and calculations presented in Table 3, area (*a*) has faster flowing particles whereas area (*c*) has the slowest flowing particles. Moreover, the results obtained from the experiment, including the mass flow rate at the outlet, particle velocities at various sections, friction factors as well as the velocity profile, are used as reference values to calibrate the simulation. This ensures that the simulation produces results that closely match the experimental data.

Numerical simulation of granular material flow in the heat exchanger

This section demonstrates the flow behaviour of granular materials within a heat exchanger. It details the simulation setup in STAR-CCM+, outlines the relevant physics applied in the Discrete Element Method (DEM) simulation, required for validation the simulation results against experimental data. The experimental values are used as reference points for the simulation. DAS and GAUTAM (2024) explains that when two bodies come into contact, they undergo a finite deformation. Hertz contact theory accounts for these deformations when they occur under external loading. As stated by THORNTON et al. (2013) Hertz-Mindlin (also referred to as no-slip model) is a standard model used to describe interactions between particles and their surrounding geometry. This model provides an effective and accurate method for calculating contact

forces between particles and geometrical surfaces (SHI et al. 2024). As stated by LI et al. (2023), this model is a foundation in DEM analysis.

The main forces in DEM analysis are:

– static friction coefficient;
– coefficient of rolling resistance;
– normal restitution coefficient;
– tangential restitution coefficient.

These forces are determined through the experiment. The static friction coefficient μ_s depends on angle of repose and is given by formula, Equation 1:

$$\mu_s = \tan \theta,$$

where:

μ_s – the static friction coefficient,
θ – the angle of repose (through the experiment, it has been found to be 15°).

Therefore:

$$\mu_s = \tan 15 = 0.268.$$

The rolling resistance coefficient , calculated in the previous section is 0.001.

Restitution coefficients as stated by WANG et al. (2024), is a very important particle property, especially in granular material simulation, where it governs the kinetic energy loss when particles interact through collisions. AHMAD et al. (2016) adds that this parameter describes the amount of energy that is lost during contact in particle dynamic collisions. The parameter ranges between 0 and 1, where 0 indicates complete energy loss and 1 indicates no energy loss. The values used in the model are discussed later.

Model geometry and meshing

Figure 10 shows the isometric view and the meshed view of the heat exchanger that is used for the simulation. The main geometrical parameters of the heat exchanger are an overall length of 430 mm, thickness 80 mm and width 200 mm. The geometry surfaces were split by patch into the heater elements, inlet, outlet and walls. The geometry has five hollow secular sections at different locations as shown in Figure 10. An automated mesh with the selected Meshers of Surface Remesher, Automatic Repair and Polyhedral Mesher was used to mesh the heater geometry. The base size of the mesh was selected as 0.01 m with a Target Surface Size (percentage of Base as 45%). The model contains a number of 35,480 polyhedral cells.

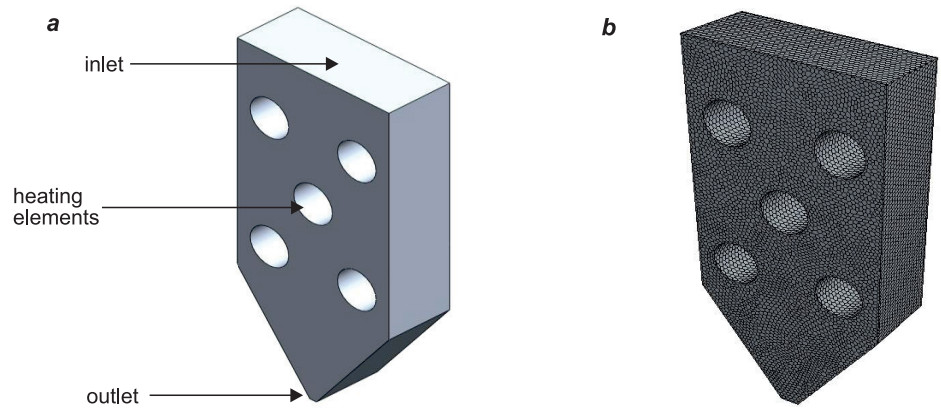

Fig. 10. Wedge-shaped heat exchanger (hopper) geometry: *a* – Isometric view, *b* – meshed view

Continua physics

A physics continuum comprises of several physics' models, including material models, flow solvers of choice and other relevant models. Every physics continuum denotes a single material that exists in every area covered by the continuum. For this simulation, the required physics models in the continuum are:

– Gas;
– Segregated Fow;
– Gradients;
– Three Dimensional;
– Constant Density;
– Implicit Unsteady;
– Laminar (Viscous regime);
– Gravity;
– Lagrangian Multiphase;
– Discrete Element Model (DEM);
– Multiphase Interaction;
– Solution Interpolation.

DEM (Lagrangian Multiphase) model

A Lagrangian Multiphase model is used to define the interaction between the discrete phase of solid granular particles and the continuous background phase of the gas domain within the heater geometry. The granular particles are chosen from the Lagrangian phases, using the following models:

– DEM Particles (Particle type);
– Pressure Gradient Force (selected automatically);
– Spherical particles (particle shape);
– Solid (Material);
– Constant Density;
– DEM Trap Walls (Optional models).

The selected material is silicon with the calculated density of 3628.14 kg/m^3, and the Poisson's ratio of 0.28. The Lagrangian multiphase is set to be bounded by stainless steel walls (just as with the experiment).

Multiphase interaction

This continua model describes the interactions between the Lagrangian phases and the boundary conditions. The boundary interactions defined for this model are the particle-to-particle and particle-to-wall interactions. The following models were selected within the interaction:

– DEM Phase Interaction;
– Hertz Mindlin;
– Rolling Resistance.

Hertz-Mindlin parameters (the friction coefficients), are the key parameters that affect the macroscopic behaviour of the non-cohesive bulk material (WENSRICH, KATTERFELD 2012). These parameters need to be calibrated well in the simulation based on the experimental data, to give more realistic results corresponding to the experimental data. The obtained values for the Hertz--Mindlin frictional factors through the experiment are:

– Static friction coefficient (obtained as 0.268);
– Coefficient of rolling resistance (obtained as 0.001).

Restitution coefficients were varied between 0.4 and 0.65 based on studies (that involve similar material as Silicon) conducted by QIN et al. (2019) (assumes 0.77), JIANG et al. (2025) (assumes 0.5), STARON, HINCH (2007) (assumes 0.5), GRIMA, WYPYCH (2011) (assumes 0.55). Through trial and error, the normal and tangential restitution coefficients were set to 0.5, which agrees with JIANG et al. (2025), who uses material with same diameter and the particle density as this study.

Regions

The faces of the heat exchanger are assigned to regions. Only the inlet and the outlet boundaries are set to pressure inlet and outlet.

Field functions

Field functions allow for access to fields such as vector or scalar data evaluated at boundary faces or cells. Field functions may be used to specify boundary and regions values. The following are the field functions that have been set for this simulation: particle flow_rate (12/${TimeStep}) and particles to retain (95,000). The particle flow rate function stated that 12 particles are injected into the geometry per each TimeStep set up to 0.01 s.

Reports

Reports to count the number of particles maintained inside the heat exchanger, the mass flow rate of particles at the outlet, and the particles to be replaced have been created. These reports are then monitored and plotted against time.

Injector

Particles enter the fluid continuum by injectors. The injectors determine where, in what direction, and at what frequency the particles enter the domain, whereas the Lagrangian phase specifies which particles enter and how they behave. A part injector was selected for the injection of this simulation. This part injector generates a cloud of injection points that are positioned in accordance with the geometry of the parts that are selected. Figure 11 shows the conditions and values that apply to the assigned Lagrangian phase, which in this case is silicon particles. The values have been set as follows, the particle diameter is 0.004 m, particle flow rate is constant and is defined by a field function ${Particle replacement_rateReport} with dimensions as per time.

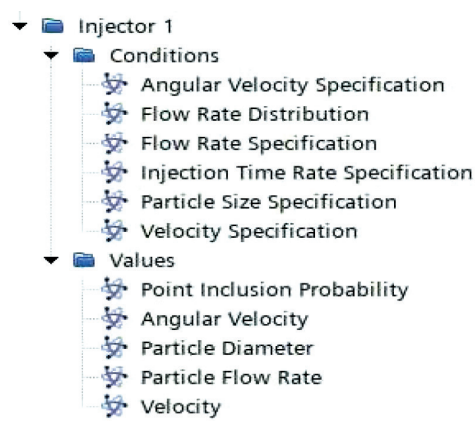

Fig. 11. Injection manager conditions

Results and discussion of model's flowability simulation

Initially the outlet is closed to let the geometry be filled with the particles. The inlet is then opened to let the particles flow in. These are 4 mm diameter silicon particles are subsequently given an initial velocity of 0.5 m/s. Figure 12 shows the filing process of the particles into the heat exchanger.

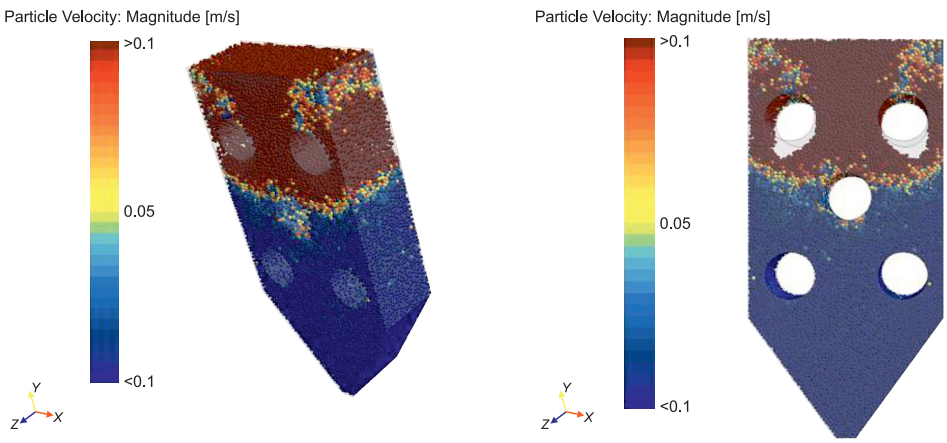

Fig. 12. Particle filling with the outlet closed

To fill up the heat exchanger, the inlet is opened while the outlet is left closed till particles completely fill it up. The number of particles is then counted using the Particle count report. The counted number of particles retained in the heat exchanger is averaged to 94,650 as shown in Figure 13. This is the number of particles when the flow is balanced. For the particle flow to be balanced, the heat exchanger's outlet is opened to let the particles flow out, while simultaneously filling through the inlet. The balanced flow is attained when there is a constant number of particles maintained in the heat exchanger without creating any empty spaces. From Figure 13, it is clear that a balanced flow is attained at about 2.5 seconds.

A replacement report and monitor are also created to determine the number of particles needed to be replaced (move their position) in the heat exchanger to keep it balanced. Figure 14 shows a relationship between the particle replacement rate into the geometry and time. Figure 13 and Figure 14 show an inverse relationship, where the replacement rate decreases with an increase in the particles being counted in the heat exchanger. This trend significantly shows that the number of particles needed to be replaced in the heat exchanger will decrease when the number of particles counted in it is getting closer to 94,650. When the number of particles decreases, the replacement rate monitor will increase to meet the number of particles needed. Once the replacement rate

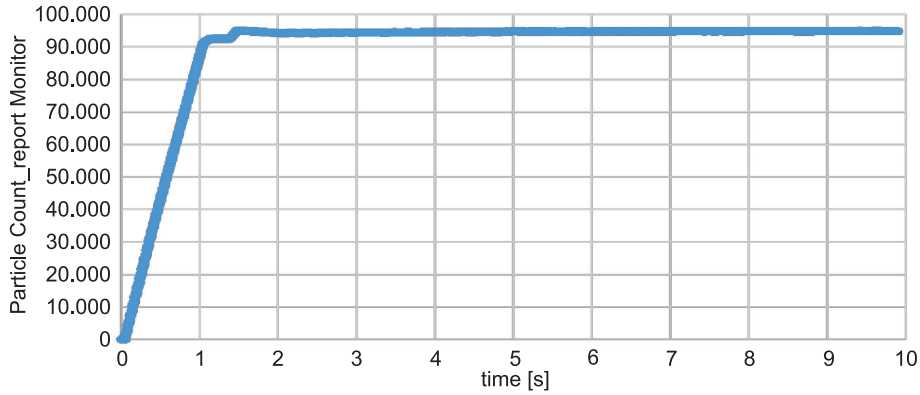

Fig. 13. Number of particles counted in the heat exchanger for a given time

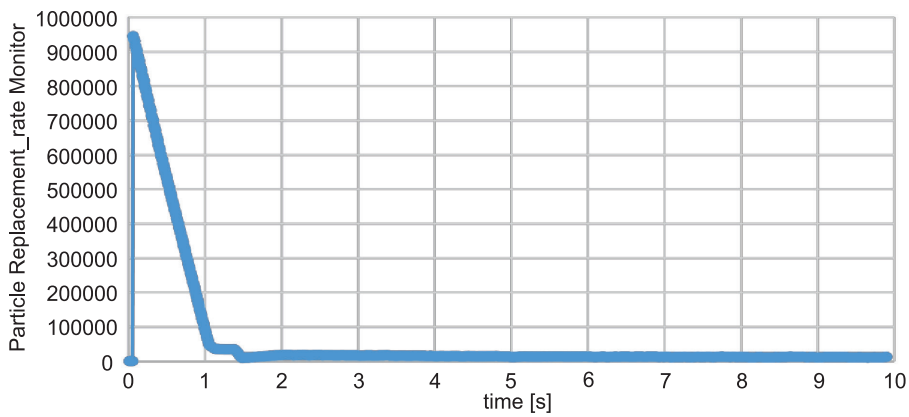

Fig. 14. Relationship between particle replacement rate and time

monitor and the particle count report are stabilized, the flowrate of the particle into and out of the geometry will also stabilize.

When the replacement rate monitor and particle count report have stabilized, the particle flow rate entering and exiting the heat exchanger also stabilizes. Figure 15 illustrates a balanced particle flow within the heat exchanger. Particles in red represent fast flow with velocities exceeding 0.009 m/s, while particles in blue indicate slower flow with velocities near 0 m/s. It is also clear in Figure 15 that particle flow is most intense at the centre of the heat exchanger and diminishes toward the sidewalls.

Additionally, a report was generated to monitor the mass flow rate at the heat exchanger's outlet. Figure 16 shows the mass flow rate of the particles at the outlet of the heat exchanger per unit time. The average mass flow rate of the particles was obtained as 133.16 g/s as shown by the average particle mass flow legend in Figure 16.

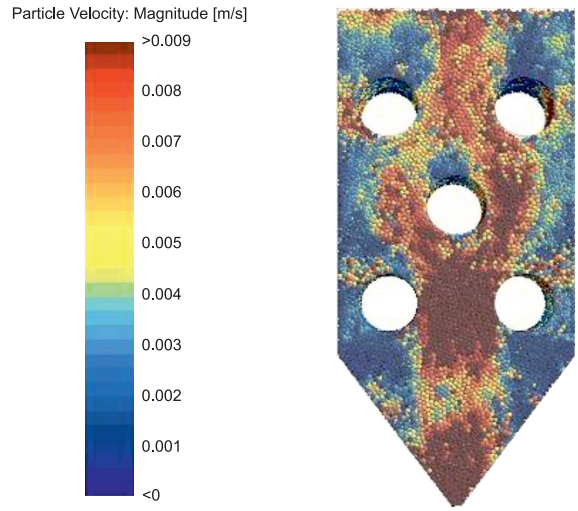

Fig. 15. Balanced flow in the heat exchanger

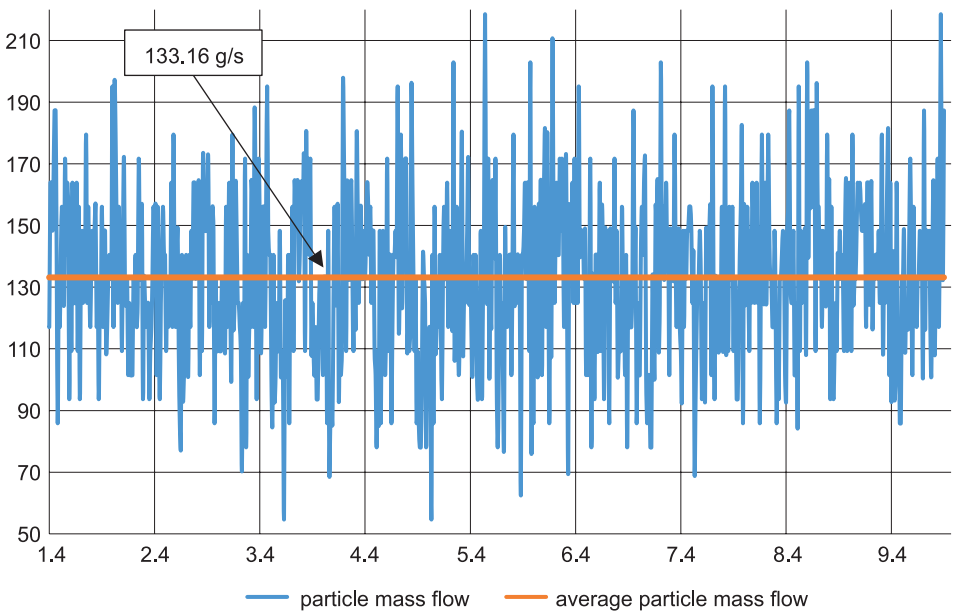

Fig. 16. Particle mass flow rate at the outlet of the heat exchanger

Model validation

The validation of the simulated results confirms that the model's geometry is identical to that of the experimental apparatus. The model exhibits identical mechanical and geometrical properties to those of the experiment. The fit-for-purpose CFD model was successfully validated and can further be applied for further studies on the performance of granular material heat exchangers. Through the experiment and an assumption of the packing density of 63%, the calculated number of particles was 95,413, however, through simulation it has been obtained as 94,650, which is reasonably close, 0.8%. Just as with the experiment, velocities at different sections of the model were determined. Areas *a* to *d* are named in the same order as presented shown in Figure 17 and in Table 2. The simulated velocities are compared to the experimental data and presented in Table 4. It is clear from the comparison that the velocities are close just as expected. The calculated mass flow of the particles through the experiment is 140.85 g/s, whereas through the simulations it has been obtained as 133.16 g/s.

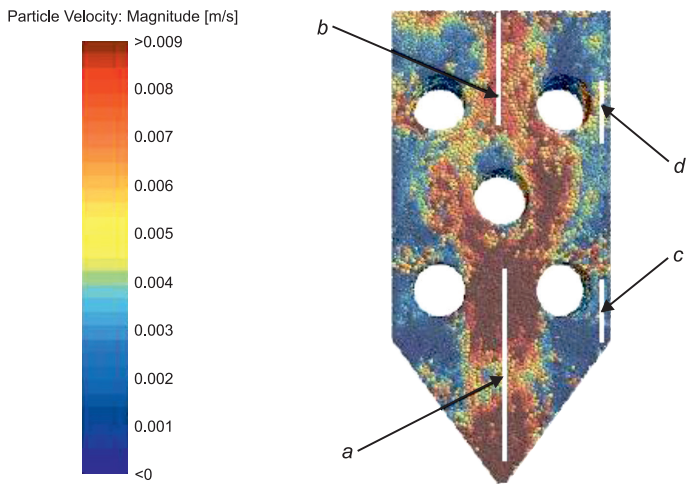

Fig. 17. Naming of areas in the model for velocity comparison between the experiment and the simulation (description in text)

Table 4

Particle velocity comparison between the experiment and the simulation

Area	Simulated velocity range [mm/s]	Experimental velocity [mm/s]
a	9 to 11	9.09
b	6 to 7	6.83
c	1 to 2	1.63
d	5 to 6	5.47

Through inspection, it is observed that velocity profiles of particles flowing through the heat exchanger are also similar. Figure 18 shows that highest particle velocities are experienced at the centre of the heat exchanger.

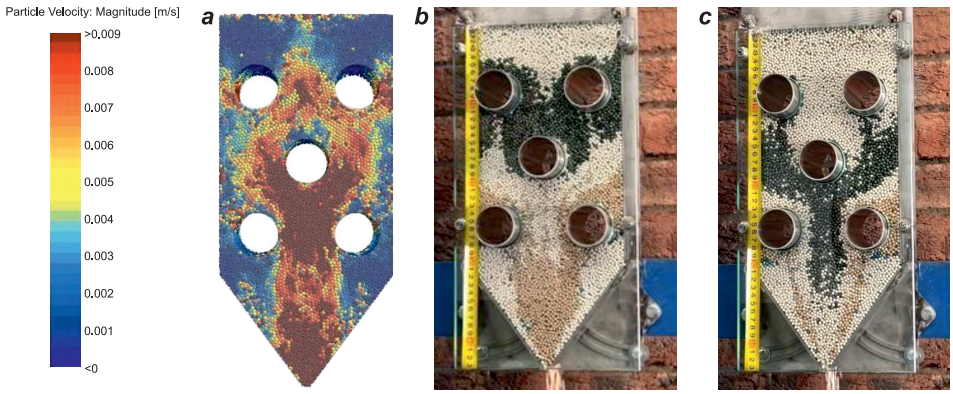

Fig. 18. Velocity profile: *a* – simulated model, particles position in two-time instances, *b* and *c* – experimental model

Conclusion

Through the successful model validation process was proved the main objective of this work, namely "CFD technology, in this case (STAR CCM+) can be successfully employed in optimizing the heat exchanger flowability by evaluation of granular material flow through changing its geometry and that of the heating elements". Additionally, was observed the following:

– The heat exchanger performance is greatly dependant on the geometry of the heating elements and their installation configuration as well as the size of the outlet.

– To maximise performance, the particles must flow uniformly through the exchanger and there must not be any blockages to the flow.

– The contact area (heating element and material) must be as large as possible with particle velocities passing the heating elements at uniform velocities.

– The efficiency of the heat exchanger strongly depends on the type of material, especially the material flowability parameter.

Acknowledgment

The authors would like to acknowledge the experimental support provided by Drytech International (Pty) Ltd company, especially the design and construction of the test rigs and performing the experimental measurements. They also would like to acknowledge the support provided by Aerotherm (Pty) Ltd company in development of numerical model using STAR CCM+ software.

References

AELA P., ZONG L., ESMAEILI M., SIAHKOUHI M., JING G. 2022. *Angle of repose in the numerical modeling of ballast particles focusing on particle-dependent specifications: Parametric study*. Particuology, 65: 39-50. https://doi.org/10.1016/j.partic.2021.06.006

AHMAD M., ISMAIL K.A, MAT F. 2016. *Impact models and coefficient of restitution: A review*. ARPN Journal of Engineering and Applied Sciences, 11(10): 6549-6555.

BALEVIČIUS R., KAČIANAUSKAS R., MRÓZ R., SIELAMOWICZ I.Z. 2011. *Analysis and DEM simulation of granular material flow patterns in hopper models of different shapes*. Advanced Powder Technology, 22(2): 226-235. https://doi.org/10.1016/j.apt.2010.12.005

BEAKAWI AL-HASHEMI H.M., BAGHABRA AL-AMOUDI O.S. 2018. *A review on the angle of repose of granular materials*. Powder Technology, 330: 397-417. https://doi.org/10.1016/j.powtec.2018.02.003

BOATENG A.A. 1998. *Boundary layer modeling of granular flow in the transverse plane of a partially filled rotating cylinder*. International Journal of Multiphase Flow, 24(3): 499-521. https://doi.org/10.1016/S0301-9322(97)00065-7

FERNANDES A.C.S., GOMES H.C., CAMPELLO E.M.B., PIMENTA P.M. 2017. *A fluid-particle interaction method for the simulation of particle-laden fluid problems*. Proceedings of the XXXVIII Iberian Latin American Congress on Computational Methods in Engineering, no. January. https://doi.org/10.20906/cps/cilamce2017-0139

DAS S.K., GAUTAM S.S. 2024. *A comprehensive isogeometric analysis of frictional Hertz contact problem*. Tribology International, 200: 110078. https://doi.org/10.1016/j.triboint.2024.110078

GRIMA A.P., WYPYCH P.W. 2011. *Development and validation of calibration methods for discrete element modelling*. Granular Matter, 13(2): 127-132. https://doi.org/10.1007/s10035-010-0197-4

HAO T. 2008. *Viscosities of liquids, colloidal suspensions, and polymeric systems under zero or non-zero electric field*. Advances in Colloid and Interface Science, 142(1-2): 1-19. https://doi.org/10.1016/j.cis.2008.04.002

JIAN B., GAO X. 2023. *Investigation of spherical and non-spherical binary particles flow characteristics in a discharge hopper*. Advanced Powder Technology, 34(5): 104011. https://doi.org/10.1016/j.apt.2023.104011

JIANG H., NIE J., DEBANATH O.C., LI Y. 2025. *Dynamic column collapse of dry granular materials with multi-scale shape characteristics*. Computers and Geotechnics, 177(Part A): 106873. https://doi.org/10.1016/j.compgeo.2024.106873

KALLUS Y. 2016. *The random packing density of nearly spherical particles*. Soft Matter, 12(18): 4123-4128. https://doi.org/10.1039/c6sm00213g

KHAN K.U.J., XU W.J. 2024. *The influencing factors and mechanisms of granular flow dynamics*. Powder Technology, 449: 120376. https://doi.org/10.1016/j.powtec.2024.120376

KUMAR N. 2023. *Chapter Eight – Fundamentals of conveyors*. In: *Transporting operations of food materials within food factories*. Eds. S.M. Jafari, N. Malekjani. Woodhead Publishing, Sawston, p. 221-251. https://doi.org/10.1016/B978-0-12-818585-8.00003-9

LI J., PENG F., LI H., RU Z., FU J., ZHU W. 2023. *Material evaluation and dynamic powder deposition modeling of PEEK/CF composite for laser powder bed fusion process*. Polymers, 15(13): 2863. https://doi.org/10.3390/polym15132863

MatWeb. 2024. *Silicon, Si*. Retrieved from https://www.matweb.com/search/datasheet.aspx?matguid=7d1b56e9e0c54ac5bb9cd433a0991e27&n=1&ckck=1

McGlinchey D. 2008. *Bulk solids handling: equipment selection and operation*. Blackwell Publishing, Hoboken. https://doi.org/10.1002/9781444305449

Mindlin R.D., Deresiewicz H. 1953. *Elastic spheres in contact under varying oblique forces*. Journal of Applied Mechanics, 20(3): 327-344. https://doi.org/10.1115/1.4010702

Qin R., Fang H., Liu F., Xing D., Yang J., Lv N., Chen J., Li J. 2019. *Study on physical and contact parameters of limestone by DEM*. IOP Conference Series: Earth and Environmental Science, 252(5): 052110. https://doi.org/10.1088/1755-1315/252/5/052110

Santomaso A., Lazzaro P., Canu P. 2003. *Powder flowability and density ratios: The impact of granules packing*. Chemical Engineering Science, 58(13): 2857-2874. https://doi.org/10.1016/S0009-2509(03)00137-4

Shi J., Shan Z., Yang H. 2024. *Research on the macro- and meso-mechanical properties of frozen sand mold based on Hertz-Mindlin with Bonding model*. Particuology, 88: 176-191. https://doi.org/10.1016/j.partic.2023.08.019

Siemens Digital Industries Software. 2023. *Simcenter STAR-CCM+ User Guide, version 2302*. p. 5184-5218. Retrieved from https://docs.sw.siemens.com/documentation/external/PL20200805113346338/en-US/userManual/userguide/html/STARCCMP/GUID-28A739CF-6DE2-4D87-B582-E390B522011C.html#

Stanley-Wood N. 2009. *Bulk powder properties: instrumentation and techniques*. In: Bulk Solids Handling: Equipment Selection and Operation. Ed. D. McGlinchey. Blackwell Publishing, Hoboken, p. 1-67. https://doi.org/10.1002/9781444305449.ch1

Staron L., Hinch E.J. 2007. *The spreading of a granular mass: Role of grain properties and initial conditions*. Granular Matter, 9(3-4): 205-217. https://doi.org/10.1007/s10035-006-0033-z

Tahmasebi P. 2023. *A state-of-the-art review of experimental and computational studies of granular materials: Properties, advances, challenges, and future directions*. Progress in Materials Science, 138: 101157. https://doi.org/10.1016/j.pmatsci.2023.101157

Thornton C., Cummins S.J., Cleary P.W. 2013. *An investigation of the comparative behaviour of alternative contact force models during inelastic collisions*. Powder Technology, 233: 30-46. https://doi.org/10.1016/j.powtec.2012.08.012

Wang G., Niu Z., Liu Y., Cheng F. 2024. *Two novel semi-analytical coefficients of restitution models suited for nonlinear impact behavior in granular systems*. Powder Technology, 452: 120501. https://doi.org/10.1016/j.powtec.2024.120501

Wensrich C.M., Katterfeld A. 2012. *Rolling friction as a technique for modelling particle shape in DEM*. Powder Technology, 217: 409-417. https://doi.org/10.1016/j.powtec.2011.10.057

Zhang P., Bi Z., Yu H., Wang R., Sun G., Zhang S. 2023. *Effect of particle surface roughness on the flowability and spreadability of Haynes 230 powder during laser powder bed fusion process*. Journal of Materials Research and Technology, 26: 4444-4454. https://doi.org/10.1016/j.jmrt.2023.08.173

Zheng Q.J., Yu A.B. 2015. *Modelling the granular flow in a rotating drum by the Eulerian finite element method*. Powder Technology, 286: 361-370. https://doi.org/10.1016/j.powtec.2015.08.025